CONF-811113--46

MASTER

FUELING OF MAGNETIC-CONFINEMENT DEVICES*

S. L. Milora

Oak Ridge National Laboratory
Oak Ridge, Tennessee 37830

CONF-811113--46

DE82 004055

ABSTRACT

A general overview of the fueling of magnetic confinement devices is presented, with particular emphasis on recent experimental results. Various practical fueling mechanisms are considered, such as cold gas inlet (or plasma edge fueling), neutral beam injection, and injection of high speed cryogenic hydrogen pellets. The central role played by charged particle transport and recycle of plasma particles from material surfaces in contact with the plasma is discussed briefly. The various aspects of hydrogen pellet injection are treated in detail, including applications to the production of high purity startup plasmas for stellarators and other devices, refueling of tokamak plasmas, pellet ablation theory, and the technology and performance characteristics of low and high speed pellet injectors.

*Research sponsored by the Office of Fusion Energy, U.S. Department of Energy, under contract W-7405-eng-26 with the Union Carbide Corporation.

1. INTRODUCTION

The issue of fueling in fusion devices has recently taken on added significance as plasma densities large enough to satisfy the requirements for scientific and economic feasibility of fusion have been achieved on experimental devices that embody several of the magnetic confinement approaches. In this paper we review the experimental physics and technological aspects of this area of research with particular emphasis on the tokamak experimental results, from which we derive most of our knowledge of fueling.

The material treated only briefly here is expanded upon and complemented by several articles in this issue. A bibliography of these articles is provided.

2. PARTICLE TRANSPORT

In laboratory experiments, replenishment of the charged particles that constitute the plasma is required when the duration of the experiment exceeds the characteristic particle confinement time, $\tau_p = (1/N)(dN/dt)$, where dN/dt is the loss rate of ions from the plasma column in the absence of fuel sources. Direct and reliable measurements of τ_p as defined here are virtually impossible to perform under realistic conditions, because reflux of plasma particles and neutrals from the surrounding vacuum chamber walls gives rise to a residual source of fuel that cannot be eliminated entirely. In confinement devices where this recycling effect has been minimized, as in the Divertor and Injection Tokamak Experiment (DITE)[1] and the Poloidal Divertor Experiment (PDX),[2]

time constants of 25-50 ms have been measured in density decay experiments, giving an upper bound on τ_p for laboratory plasmas. Since discharge durations on the order of 1 s are now typical, most magnetic confinement devices routinely use external fueling, usually in the form of cold gas injection at the vacuum chamber wall, to maintain densities in the relevant range of 10^{13} cm^{-3} to 10^{14} cm^{-3}.

Apart from the question of particle confinement, the details of the fueling process in general can be learned only by comparing experimental measurements with particle transport codes. For toroidal confinement devices where magnetic field lines close upon themselves, such as tokamaks and stellarators, axisymmetric one-dimensional models are adequate to describe the transport of charged particles across the plasma column (viz., across or perpendicular to the confining magnetic field). Following Howe,[3] we write the appropriate particle diffusion equation for a single species as

$$\frac{\partial n}{\partial t} = S + \frac{1}{r}\frac{\partial}{\partial r}(r\Gamma + rnv) - \frac{n}{\tau_{\parallel}}, \qquad (1)$$

where n is the charged particle density, r is the plasma radius, S(r,t) is the volume source rate of particles from all fueling mechanisms, $\Gamma = -D(\partial n/\partial r)$ is the diffusive (cross-field) charged particle flux, and v is the optional inward neoclassical pinch velocity.[4] This term is sometimes needed to explain the rapid buildup of density in the plasma center during gas injection experiments on tokamaks.[5] The last term in Eq. (1) is included only in the so-called scrapeoff region of the plasma, where magnetic field lines terminate on the extended surfaces of

the vacuum chamber (see Fig. 1), giving rise to a depletion of charged particles. The parallel flow time $\tau_{\|}$ is roughly the average time for an ion to impact such a surface as it circles the torus along magnetic field lines at the local sound speed. In open magnetic confinement systems, the particle balance may also be described by Eq. (1) (see Ref. 6), although the parallel transport must be considered everywhere because essentially all magnetic field lines terminate on surfaces. For present systems, such as the Tandem Mirror Experiment (TMX), the parallel and radial losses are about equal in importance.[7,8]

In the main body of the plasma, diffusive losses must be balanced by the source terms locally (in steady state). While in principle it might be possible to control the shape of the plasma density profile in this way, in practice this is made difficult by the currently non-existent, perfectly flexible source term needed and by the fact that the diffusion coefficient may vary widely throughout the plasma. For tokamaks, the situation is even more complicated because the transport is observed to be anomalous; that is, the experimental measurements do not substantiate the neoclassical theory.[9] The resulting uncertainty has led to the development of several empirical transport models, none of which is totally satisfactory. For the purpose of illustration, we list only two of the proposed models for which there exists some experimental basis. According to Mercier[10] the following form for the particle diffusivity is in agreement with results from the Tokamak Fontenay-aux-Roses (TFR) and the Princeton Large Torus (PLT):

$$D = \frac{0.7 D_l D_B}{D_l + 0.7 D_B} \qquad (cm^2/s) \ ,$$

$$D_l = \frac{2.5 \times 10^{19}}{n_e q T_e^{3/4}} \qquad (cm^2/s) \ , \tag{2}$$

$$D_B = 6.25 \times 10^6 \frac{T_e}{B} \quad (cm^2/s) \ ,$$

where T_e is the electron temperature in electron volts, n_e is the electron density in (centimeters)$^{-3}$, q is the safety factor (varies from $\sim$1 to $\sim$3 from center to edge), D_B is the Bohm diffusion coefficient, and B is the toroidal magnetic field strength in gauss. The form of Eq. (2) ensures that in the main body of the plasma, where T_e and n_e are large, $D \approx D_l \ll D_B$, while in the cold, tenuous plasma edge where the transport is larger, $D \approx D_B$. There is no experimental basis for the parametric dependence given by the Bohm value, but diffusion coefficients on the order of D_B are often inferred from edge plasma measurements.[5] Another model that is frequently used for estimating the performance of future toroidal devices, such as the International Tokamak Reactor (INTOR) design,[11] relates the diffusion coefficient in the main plasma to the density and plasma radius as

$$D = \frac{1.25 \times 10^{17}}{n_e} + 5000 (r/a_s)^3 \ , \tag{3}$$

where a_s is the radius of the plasma column. These two models have in common only the inverse density dependence. The origin of this scaling derives from the observation that energy and particle confinement times

are roughly equal in tokamaks and stellarators and that for densities less than $\sim 3 \times 10^{14}$ cm^{-3}, $\tau_E \sim (a^2/4)\chi_e^{-1} = 4 \times 10^{-19}\bar{n}_e a_s^2$, where χ_e (cm^2/s) is the average electron heat diffusivity and $\bar{n}_e$ is the line-averaged electron density. This result has been demonstrated in the Alcator tokamaks at the Massachusetts Institute of Technology (MIT).[12,13]

Although these two models differ markedly in form, they give roughly equivalent values for D in the various regimes characteristic of laboratory plasmas. For typical central conditions ($r = 0$, $n_e = 5 \times 10^{13}$ cm^{-3}, $T_e \sim 1$ keV, $q = 1$), $D \approx 2000$-2500 cm^2/s, while near the plasma boundary ($r \approx a$, $n_e \approx 1 \times 10^{13}$ cm^{-3}, $T_e \sim 100$ eV, $q = 3$), $D \approx 10{,}000$-$20{,}000$ cm^2/s. The larger values are thought to be due to a kind of turbulence commonly associated with large density fluctuations observed near the limiter radius.[14,15] The large variation in D across the plasma column helps to illustrate the important difference between edge and central fueling. If fuel is deposited in the central plasma region, then we expect a replacement rate based on the time required for charged particles to diffuse across the plasma radius using the central value for D, viz., $\tau_p = a^2/4D$ (Ref. 16) ≈ 100 ms for $a = 30$ cm. On the other hand, if the fuel is added near the plasma edge, as in gas injection or recycle, then the corresponding fueling rate must be larger to offset the combined effects of large D and a smaller diffusive scale length.

Recent experiments performed on the TMX device[8] indicate that radial particle losses for tandem mirror systems may, within experimental uncertainties, be ascribed to resonant-neoclassical diffusion, and consequently transport codes based on theory might accurately model future experiments in which radial transport is expected to be dominant.

For present TMX parameters, particle confinement times of ∿5 ms have been reported.[8] In these devices, external fueling is required not only to maintain the plasma density at elevated values but also to prevent the onset of end cell microinstabilities that degrade the central cell confinement.[17]

3. GAS INJECTION AND RECYCLING

Broadly speaking, gas injection and recycling are similar processes in that the hydrogen fuel originates from or near the metallic surfaces that surround or are in direct contact with the plasma (see Fig. 1). The results of a transport code calculation[3] illustrating the various terms in Eq. (1) for this type of fueling are displayed in Fig. 2 for the moderate-size Impurity Study Experiment (ISX-B) limiter plasma ($a_s \approx 30$ cm). As mentioned above, the source term is peaked in the outer plasma region where confinement is poor, but the profile is nevertheless broad enough to fuel a sizable fraction of the plasma. For this example, the Ware pinch term is responsible for balancing the diffusive losses from the plasma center.

The mechanism by which gas can penetrate the hot plasma is multiple charge exchange collisions starting from the ∿2- to 6-eV Franck-Condon neutrals that are formed by dissociation of molecules and molecular ions in the plasma edge.[18] The internal source term is usually calculated by solving the Boltzmann neutral transport equation[19] or by employing a Monte Carlo technique[20] to track the successive charge exchange events until the process is terminated by electron impact ionization. Some

fraction of the hot charge exchange flux can illuminate the device walls, giving rise to a direct reflection component,[21] trapping and diffusion in the wall, and desorption and release of cold gas.[22] Additional recycling of cold gas and hot atoms can occur at the limiter as a result of the concentrated flux of charged particles there [the retention of hydrogen in stainless steels saturates at a fluence of $\sim 10^{18}$ cm^{-2} (see Ref. 23)]. In principle, all of the above aspects of wall recycle can be added to the basic plasma particle transport code to obtain a self-consistent description of the fueling process. Such an exercise was first undertaken by Howe.[3] He concludes that, in limiter plasmas, recycling of particles in the plasma boundary accounts for $\sim$90% of the fueling.

The relationship between the global recycle fraction R, the particle confinement time τ_p, and the fueling rate ϕ can be determined in an approximate sense by integrating Eq. (1) over the plasma volume inside the limiter radius. Writing the diffusive loss of ions at the edge as N/τ_p and the total source rate as a sum of the external gas injection ϕ_g and the recycle contribution $\phi_R = RN/\tau_p$, we find

$$\frac{dN}{dt} = -\Gamma A\Big|_{a_s} + \phi_g + \phi_R$$

$$= -\frac{N}{\tau_p} + \phi_g + R\frac{N}{\tau_p} = -\frac{N}{\tau_p^*} + \phi_g \,, \qquad (4)$$

where $\tau_p^* = \tau_p/(1 - R)$ is the density decay time constant measured in the absence of external fueling. For a given steady-state density or a given rate of density rise, large recycle fractions reduce the required

rate of external fueling. This can be seen by comparing the ISX-B simulation of Fig. 2 with the data of Fig. 3(a). In the simulation, a total source of 3.5×10^{21} ions/s, corresponding to an equivalent 50 torr·ℓ/s of H_2 gas, is required to maintain a steady-state density. Experimentally it is found that a gas feed rate of only 10 torr·ℓ/s will support a net density increase (corresponding to a gain of ~3 torr·ℓ/s). These values suggest an overall recycle fraction greater than 85%.

Additional details of the recycling process can be learned from spectroscopic measurements of hydrogen light emissions, such as those performed on the Alcator-A device by Marmar.[24] As shown in Fig. 4, H_α light emission produced by excitation of neutrals and molecular ions is highest near the limiter location. These data indicate that recycling is a significant, if not a dominant, fueling mechanism and that the effect occurs predominantly at surfaces in direct contact with the plasma. Isotopic changeover experiments, such as those described by Roberto et al. and Clausing et al. in this issue, indicate the importance of wall retention in the fueling process. These studies show that rapid recycling causes the working gas to be replaced as the majority plasma component by the wall constituent within a few particle confinement times, even during gas injection of the working gas.

In devices with magnetic divertors, such as the PDX tokamak,[2,25] the magnetic field can be configured to shape the scrapeoff plasma so as to locate the "limiter" in a remote pumping chamber that prevents most of the neutralized parallel ion flux from reentering the plasma. Global recycling for these devices can be made small ($R \approx 0.5$) in

comparison to limiter plasmas.[26] Gas injection is an inefficient fueling mechanism in such devices because a significant amount of fuel can be ionized in the scrapeoff plasma and swept into the divertor pumping chamber, where it is lost from the system. This is illustrated in Fig. 5 by a comparison of the steady-state fueling rate ϕ_g and the corresponding values of N/τ_p^* determined from density decay experiments on PDX. The difference, which has been interpreted as the amount of fuel ionized and then lost in the scrapeoff plasma, is an increasing function of plasma density. This illustrates one of the limitations of gas injection. As the density or plasma size is increased, the source term will be peaked progressively further from the plasma center owing to the fact that the neutral particle mean free path against electron impact ionization decreases at higher density.

Despite its limitations, gas injection is the simplest form of fueling and is routinely used on toroidal and open confinement devices alike (see the articles by H. F. Dylla and E. B. Hooper et al. in this issue). A practical system usually consists of one or more magnetic or piezoelectric valves that can be feedback-controlled or preprogrammed to maintain a given plasma density waveform. Response times on the order of ∿1 ms are typical, and maximum throughput levels range up to ∿200 torr·ℓ/s.

4. PELLET INJECTION

Plasma fueling by injection of frozen hydrogen pellets at high speed has been proposed to overcome the limitations or inflexibility of

edge fueling.[28] A neutral pellet will penetrate the confining magnetic fields and, if given a high enough speed, will reach the plasma center before evaporation in the intense plasma heat is complete. For laboratory plasmas, a pellet size of 1 mm and a speed range of 1000 m/s are considered adequate for central penetration. Exploratory pellet fueling studies have been performed in this parameter range on a number of tokamaks, including the Oak Ridge Tokamak (ORMAK),[29] ISX-A,[30] ISX-B,[31] PDX,[32] and, more recently, ASDEX[33] and the Wendelstein VII-A stellarator. Although a factor of 10 or higher increase in velocity is projected for central penetration in fusion reactor plasmas, a significant fraction of the plasma volume (~70%) can nevertheless be directly reached by pellets with the technically feasible speed of 2 km/s (see the article by S. E. Attenberger et al. in this issue).

The plasma source term S(r,t) for pellet injection is obviously related to the rate at which the surface of the moving pellet evaporates; as in the case of gas injection, we must rely on theory for this information. One pellet ablation model in particular has been successful at predicting the penetration distance observed in the ORMAK, ISX, and PDX experiments. This is the so-called neutral gas shielding model,[34-39] which derives its name from the hypothesis that hydrogen gas evolves from the surface and shields the pellet by absorbing the energy of the hot streaming plasma electrons through consecutive inelastic collisions (ionization and electronic excitation). In its basic form, this model relates the local source term dN/dt (atom-equivalent/s) to the plasma parameters and pellet radius by the approximate expression from Ref. 36 (for hydrogen)

$$\frac{dN}{dt} = 2\pi_s{}^0 r_p^2 \frac{dr_p}{dt} = 2.8 \times 10^{15} n_e^{1/3} T_e^{1.64} r_p^{4/3} , \qquad (5)$$

where n_s^0 is the molecular number density of the solid and r_p is the pellet radius in centimeters. This differential equation must be solved at each location in the plasma to keep track of the diminishing pellet radius, but if the injection velocity is high enough to permit penetration to the plasma center, the strong electron temperature dependence will ensure a centrally peaked ion source term.

A comparison of this model with the experimental measurement of the line density increase during injection of a single 1-mm hydrogen pellet into PDX is shown in Fig. 6. The H_α signal records the time history of the hydrogen light emitted from the cloud of neutrals surrounding the pellet, and its duration is a measure of the evaporation time. From a time-of-flight analysis we estimate a penetration of ≈33 cm into the plasma, which has a minor radius of ≈38 cm. The theoretical pellet lifetime and the plasma line density increase constructed from the calculated ablation rate are in good agreement with the measurements. The density profile measurements displayed in Fig. 7 illustrate how pellet injection or central fueling can transform a "flat" profile, as produced by gas injection, into one that is centrally peaked. Accordingly, pellet injection appears to be more efficient than cold gas injection because the problem of ionization of fuel in the edge and the consequent rapid loss of plasma, as discussed in Sec. 3, are apparently eliminated.

The practical embodiment of pellet fueling is the equipment that produces and accelerates frozen hydrogen isotope pellets with the size, speed, and repetition rate that are relevant to present and future fusion devices.[11] Almost every imaginable technique has been proposed to fabricate and accelerate the cryogenic pellets. Liquid droplet generators,[40,41] which were developed at the University of Illinois, form a stream of condensed hydrogen at the outlet of a liquid-helium-cooled heat exchanger. The jet is broken into controlled droplets by the action of acoustic waves excited by a piezoelectric transducer that is coupled to the exit nozzle. Although large (1-mm) pellets at a feed rate of ∿100 pellets/s (∿40 torr·ℓ/s equivalent) can be produced, their velocity is limited to ∿100 m/s by the low pressure gas dynamic drag technique employed for acceleration.

Higher velocities have been achieved with gun-type devices,[42] such as the one illustrated schematically in Fig. 8. This device forms a single frozen plug in situ and transports it to a miniature gun mechanism where a puff (∿10 torr·ℓ) of moderate pressure (∿30-bar) helium propellant accelerates the pellet to ∿1000 m/s in a 17-cm gun barrel insert. Pellets as large as 1.6 mm have been produced in the original single-pellet device, and this technique has been extended to multipellet capability with a 4-barrel injector developed at Oak Ridge National Laboratory (ORNL) for use on PDX.[43] A repetitive device based on this principle will use a continuous extrusion process to feed material to the repeating gun mechanism.

Solid hydrogen extrusion appears to be the most practical way to supply the large amounts of material required in a steady-state system.

Frozen hydrogen is soft (~5-bar tensile strength) and can be readily extruded at high rates from a laboratory scale press. The extruder illustrated in Fig. 9 can feed a 1-mm-diam filament at up to 15 cm/s to the acceleration stage of the ORNL prototype centrifugal pellet injector. An advarced system based on this principle is being developed to extend the velocity performance to 1000 m/s.

Finally, low speed pellet injection has been used on a number of confinement devices to produce high purity startup plasmas. In the system used on the Doublet III tokamak,[44] a pellet is cut from an extruded rod and ejected at 15 m/s by a solenoid launcher. As the pellet reaches the centerline of the vacuum vessel, it is quickly ionized by initiating the tokamak plasma discharge around it, thereby producing a plasma with higher density and higher purity than can be achieved using prefill gas only.[45] For currentless operation, the staged laser irradiation technique described by Pechacek et al.[46] illustrated in Fig. 10 can be used to produce warm, fully ionized, pure hydrogen plasmas.

5. NEUTRAL BEAM INJECTION

Strictly speaking, the injection of intense beams of neutral atoms is a method for heating rather than fueling fusion plasmas (see the article by J. H. Fink in this issue and Ref. 47). At injection energies of several tens of kilo-electron-volts, the atomic beam can penetrate a substantial distance across the confining magnetic fields before

ionization by and subsequent slowing down on the parent plasma particles is complete. In tokamaks, record ion temperatures have been achieved by application of several megawatts of neutral beam power.

Mirror systems rely on this technique to fuel and heat the end plug plasmas to elevated densities and temperatures.[48] A typical arrangement on the TMX device is shown in Fig. 11. The 24-beam system can supply up to 500 A of equivalent atom current (~44 torr·ℓ/s) at mean energies of 13 keV into the end plug plasmas. The plugs confine the central cell plasma electrostatically, but the inevitable axial and radial particle losses from this region must be replaced by gas injection at typical feed rates of 150 torr·ℓ/s.

The principal disadvantage of this approach to fueling the core plasma of fusion devices is the large recirculating power levels required to replace the particle losses at the high energies required for full penetration. It could be argued, however, that the severity of this problem should be lessened in devices with high recycle because the makeup would be only a small fraction of the total particle loss rate. In the ISX-B beam-heated example of Fig. 3(b), the 100-A neutral beam current is equivalent to the 10-torr·ℓ/s gas fueling rate used in the ohmically heated case of Fig. 3(a). The plasma density, however, does not increase during the heating pulse and the gas puffing rate must be increased sharply to maintain the density plateau. A similar effect has also been observed on the PDX tokamak.[49] The mechanism for this apparent deterioration is not yet understood; nevertheless, an examination of Fig. 3(b) suggests the use of the less energy intensive alternatives such as gas or pellet injection.

6. CONCLUSIONS

In comparison to gas injection, pellet fueling is still in the developmental and exploratory stages. Future fusion devices are expected to use a combination of the two techniques. The method emphasized will depend not so much on fueling considerations but rather on the method chosen for particle exhaust and impurity control. If the magnetic divertor option is selected, then pellet fueling will most likely play a central role. If, on the other hand, the more economical, high recycle limiter option proves viable, then the small amount of makeup fuel required could be supplied by either technique.

ACKNOWLEDGMENTS

The author would like to thank H. C. Howe, W. A. Houlberg, R. P. Drake, and G. L. Schmidt for many helpful conversations throughout the course of this work.

BIBLIOGRAPHY

S. E. Attenberger, W. A. Houlberg, and S. L. Milora, "Numerical Simulation of Fueling in Tokamaks," PFWA-02

R. E. Clausing, L. Heatherly, and L. C. Emerson, "Hydrogen-Deuterium Changeover Experiments in a Plasma-Wall Interaction Simulator," PFWA-05

H. F. Dylla, "Pressure Measurement in Magnetic Fusion Devices," VFThM-01

J. H. Fink, "Neutral Beam Systems," PFTA-01

E. B. Hooper, Jr., G. Gryczowski, and R. P. Drake, "Plasma Generation in Gas Box Fueling for Tandem Mirrors," PFWA-03

J. B. Roberto, R. C. Isler, H. C. Howe, and L. E. Murray, "Hydrogen Recycling in ISX-B," PFWA-04

REFERENCES

1. S. J. Fielding and A. J. Wooton, J. Nucl. Mater. 93-94, 226 (1980).
2. D. K. Owens, V. Arunasalam, C. Barnes, M. Bell, et al., J. Nucl. Mater. 93-94, 213 (1980).
3. H. C. Howe, J. Nucl. Mater. 93-94, 17 (1980).
4. A. A. Ware, Phys. Rev. Lett. 25, 15 (1970).
5. M. H. Hughes and J. Hugill, in *Plasma Physics and Controlled Nuclear Fusion Research (Proc. 7th Int. Conf. Innsbruck 1978)*, Vol. 1, p. 457 (1979).
6. G. E. Gryczkowski and J. M. Gilmore, in *The Technology of Controlled Nuclear Fusion (Proc. 4th Topical Meeting 1980)*, CONF-801011, p. 188 (1981).
7. T. C. Simonen, Proc. IEEE 69, 935 (1981).
8. R. P. Drake, E. B. Hooper, C. V. Karmendy, S. L. Allen, et al., Lawrence Livermore National Laboratory Report UCRL-85872 (1981).
9. F. L. Hinton and R. D. Hazeltine, Rev. Mod. Phys. 48, 239 (1976).
10. C. Mercier, F. Werkoff, J. P. Morera, G. Cissoko, and H. Capes, Nucl. Fusion 21, 291 (1981).
11. W. A. Houlberg, H. C. Howe, and S. E. Attenberger, Oak Ridge National Laboratory Report ORNL/TM-7124 (1980).
12. A. Gondhalekar, R. Granetz, D. Gwinn, I. Hutchinson, et al., in *Plasma Physics and Controlled Nuclear Fusion Research (Proc. 7th Int. Conf. Innsbruck 1978)*, Vol. 1, p. 199 (1979).
13. S. Fairfax, A. Gondhalekar, R. Granetz, M. Greenwald, et al., in *Plasma Physics and Controlled Nuclear Fusion Research (Proc. 8th Int. Conf. Brussels 1980)*, Vol. 1, p. 439 (1981).

14. R. E. Slusher and C. M. Surko, Phys. Rev. Lett. 40, 400 (1978).

15. R. E. Slusher and C. M. Surko, Phys. Fluids 23, 472 (1980).

16. W. M. Stacey, *Fusion Plasma Analysis* (John Wiley, New York, 1981), p. 144.

17. R. P. Drake, T. A. Casper, J. F. Clauser, F. H. Coensgen, et al., Nucl. Fusion 21, 359 (1981).

18. D. H. McNeill, Princeton Plasma Physics Laboratory Report PPPL-1758 (1981).

19. K. Audenaerde, G. Emmert, and M. Gordinier, J. Comput. Phys. 34, 268 (1980).

20. M. H. Hughes and D. E. Post, J. Comput. Phys. 28, 43 (1978).

21. O. S. Oen and M. T. Robinson, Nucl. Instrum. Methods 132, 524 (1976).

22. K. L. Wilson, "Hydrogen Recycling Properties of Stainless Steel," to be published in J. Nucl. Mater.

23. B. S. Blewer, R. Berisch, B. M. U. Scherzer, and R. Schulz, J. Nucl. Mater. 76-77, 305 (1978).

24. E. S. Marmar, J. Nucl. Mater. 76-77, 59 (1978).

25. D. Meade, V. Arunasalam, C. Bell, K. Bol, et al., in *Plasma Physics and Controlled Nuclear Fusion Research (Proc. 8th Int. Conf. Brussels 1980)*, Vol. 1, p. 000 (1981).

26. D. K. Owens, "Divertor Scrape Off Studies," paper presented at the IAEA Technical Committee Meeting on Divertors and Impurity Control in Tokamaks, Garching, 1981.

27. S. L. Milora, J. Fusion Energy 1, 15 (1981).

28. C. T. Chang, L. W. Jørgensen, P. Neilsen, and L. L. Lengyel, Nucl. Fusion 20, 859 (1980).

29. C. A. Foster, R. J. Colchin, S. L. Milora, K. Kim, and R. J. Turnbull, Nucl. Fusion 17, 1067 (1977).

30. S. L. Milora, C. A. Foster, P. H. Edmonds, and G. L. Schmidt, Phys. Rev. Lett. 42, 97 (1979).

31. S. L. Milora, C. A. Foster, C. E. Thomas, C. E. Bush, et al., Nucl. Fusion 20, 1491 (1980).

32. S. L. Milora, G. L. Schmidt, R. Fonck, C. A. Foster, et al., Bull. Am. Phys. Soc. 25, 927 (1980) (complete paper to be published).

33. K. Büchl and G. Vlases, Bull. Am. Phys. Soc. 26, 888 (1981).

34. P. B. Parks, R. J. Turnbull, and C. A. Foster, Nucl. Fusion 17, 539 (1977).

35. D. F. Vaslow, IEEE Trans. Plasma Sci. PS-5, 12 (1977).

36. P. B. Parks and R. J. Turnbull, Phys. Fluids 21, 1735 (1978).

37. S. L. Milora and C. A. Foster, IEEE Trans. Plasma Sci. PS-6, 578 (1978).

38. P. B. Parks, Nucl. Fusion 20, 311 (1980).

39. R. P. Gilliard and K. Kim, IEEE Trans. Plasma Sci. PS-8, 477 (1980).

40. C. A. Foster, K. Kim, R. J. Turnbull, and C. D. Hendricks, Rev. Sci. Instrum. 48, 625 (1977).

41. R. P. Gilliard, K. Kim, and R. J. Turnbull, Rev. Sci. Instrum. 52, 183 (1981).

42. S. L. Milora and C. A. Foster, Rev. Sci. Instrum. 50, 482 (1979).

43. S. L. Milora, G. L. Schmidt, C. A. Foster, and T. McBride, Bull. Am. Phys. Soc. 26, 864 (1981).

44. E. R. Johnson, in *The Technology of Controlled Nuclear Fusion (Proc. 4th Topical Meeting)*, CONF-801011, p. 204 (1981).

45. F. B. Marcus, D. R. Baker, and J. L. Luxon, Nucl. Fusion 21, 859 (1981).

46. R. E. Pechacek, J. R. Grieg, M. Raliegh, A. W. De Silva, and D. W. Koopman, Rev. Sci. Instrum. 52, 371 (1981).

47. M. M. Menon, in Proc. IEEE 69, 1012 (1981).

48. R. P. Drake, G. Deis, M. Richardson, and T. C. Simonen, J. Nucl. Mater. 93-94, 291 (1980).

49. K. Bol, "Recent PDX Results," paper presented at the IAEA Technical Committee Meeting on Divertors and Impurity Control in Tokamaks, Garching, 1981.

FIGURE CAPTIONS

Fig. 1. Model of edge fueling and recycle in a contiguous limiter device. Γ^+ is the diffusive flux of ions at the limiter radius. Γ_L^+ is the parallel flux of ions incident on the limiter, which is neutralized and re-emitted as cold gas, Γ^L. Most of the gas is ionized in the plasma, but ~40% returns to the first wall as hot charge exchange neutrals, Γ^H, which give rise to a reflected hot neutral component, Γ^R, and a cold gas wall release component, Γ^D. Γ^G is the external cold gas feed. (Figure taken from Ref. 3.)

Fig. 2. At left, typical values for the source and loss terms of Eq. (1) for edge fueling in ohmically heated plasmas. At right, number balance for the volume inside radius r, where a_s, the limiter radius, is 26 cm. (Figure adapted from Ref. 3.)

Fig. 3. (a) Temporal variation of line average electron density, $\bar{n}_e$, for an ohmically heated ISX-B discharge, where ϕ_g is the gas injection rate. (b) A neutral-beam-heated discharge, where I_B is the neutral beam current.

Fig. 4. Absolute brightness of H_α light at three toroidal locations in Alcator-A. The Thomson scattering port is 90° from both limiter and gas injection port. Here, I_p is the plasma current and B is in photons/cm^2/s/sr. (Figure taken from Ref. 24.)

Fig. 5. Measurements of the gas injection rate, Γ, and apparent plasma particle loss rate, N/τ_p^*, for PDX diverted plasmas, illustrating the reduction in fueling efficiency as the plasma column density increases. (Figure courtesy of G. L. Schmidt, Princeton Plasma Physics Laboratory.)

Fig. 6. Plasma line density increase on PDX in response to single-pellet injection. The broken line represents a calculation of the neutral gas shielding model. (Figure taken from Ref. 32.)

Fig. 7. Electron temperature and density profiles before and after pellet injection into PDX. The broken line represents a calculation of the immediate post-pellet density using the neutral gas shielding model. (Figure taken from Ref. 32.)

Fig. 8. Operating principle of ORNL pneumatic hydrogen pellet injector. (Figure taken from Ref. 27.)

Fig. 9. Schematic of ORNL 30-cm centrifugal pellet injector. The high speed solid hydrogen extruder in combination with the rapidly rotating arbor produces pellets at a rate of 150 pellets/s and accelerates them to 290 m/s by centrifugal forces. (Figure courtesy of C. A. Foster, ORNL.)

Fig. 10. Holographic interferogram of expanding, fully ionized, hydrogen plasma taken 0.4 μs after a 1-kJ CO_2 laser pulse ionizes the hydrogen gas cloud produced 2 μs earlier by laser vaporization of a 1-mm cube of solid D_2. (Figure taken from Ref. 46.)

Fig. 11. Schematic of TMX showing neutral beam injection system, gas boxes, and startup plasma guns. The central cell solenoid plasma can also be fueled by gas puff valves (not shown). (Figure taken from Ref. 7.)

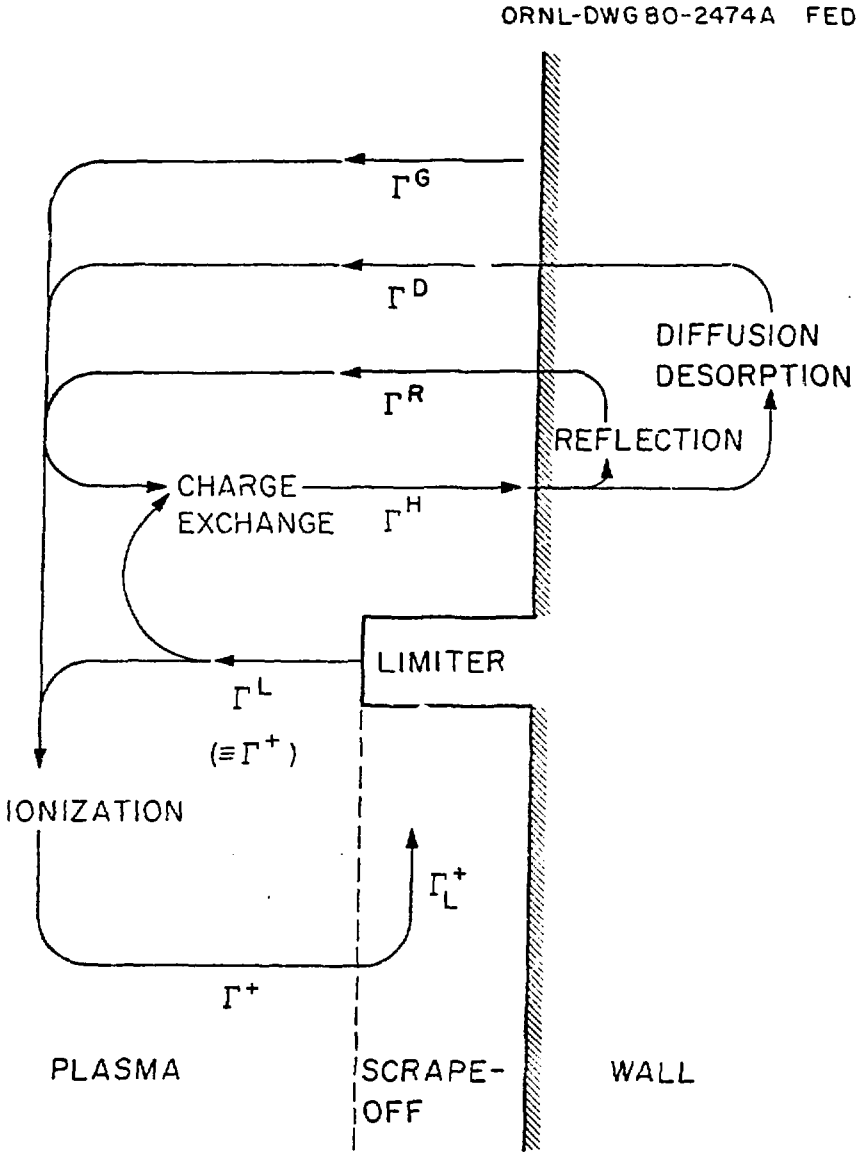
ORNL-DWG 80-2474A FED
Γ^G
Γ^D
DIFFUSION
DESORPTION
Γ^R
REFLECTION
CHARGE
EXCHANGE
Γ^H
LIMITER
Γ^L
$(\equiv \Gamma^+)$
IONIZATION
Γ_L^+
Γ^+
PLASMA
SCRAPE-
OFF
WALL

MILORA

Fig. 1

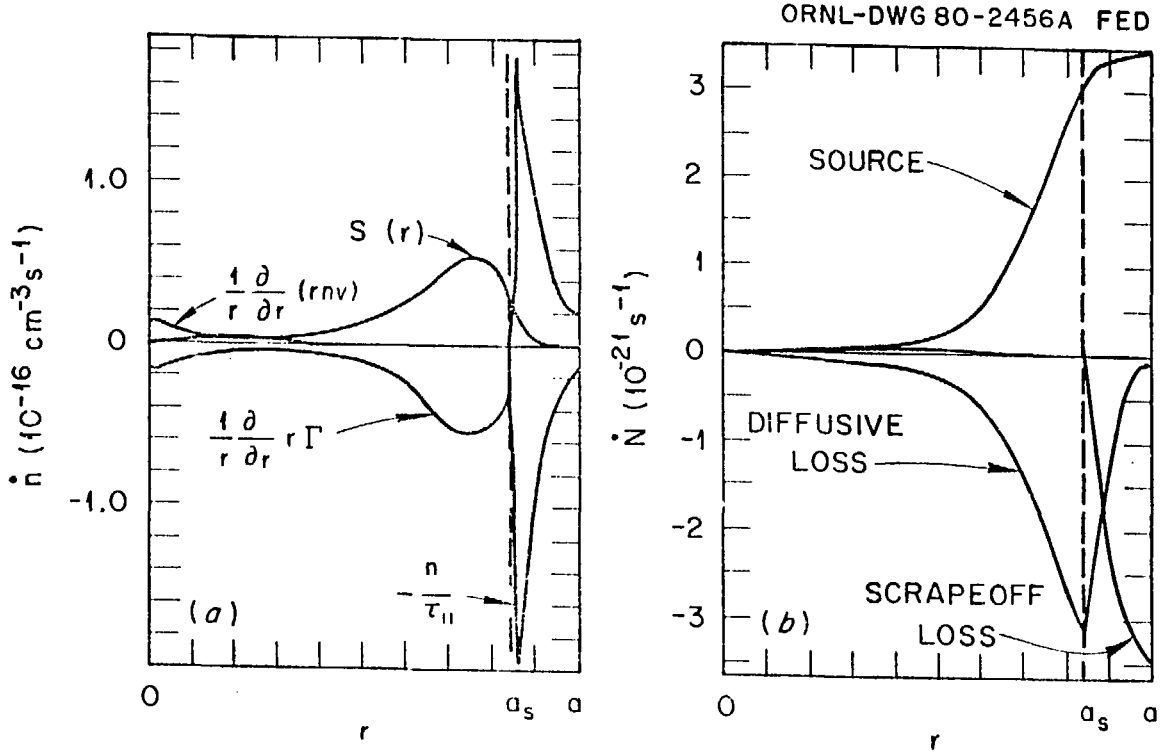
ORNL-DWG 80-2456A FED
1.0
0
-1.0
S (r)
$\frac{1}{r}\frac{\partial}{\partial r}(rnv)$
$\frac{1}{r}\frac{\partial}{\partial r} r\Gamma$
$\frac{n}{\tau_{\parallel}}$
(a)
$\dot{n}$ (10^{-16} cm^{-3}s^{-1})
0
a_s
a
r
3
2
1
0
-1
-2
-3
SOURCE
DIFFUSIVE LOSS
SCRAPEOFF LOSS
(b)
$\dot{N}$ (10^{-21} s^{-1})
0
a_s
a
r

MILORA
Fig. 2

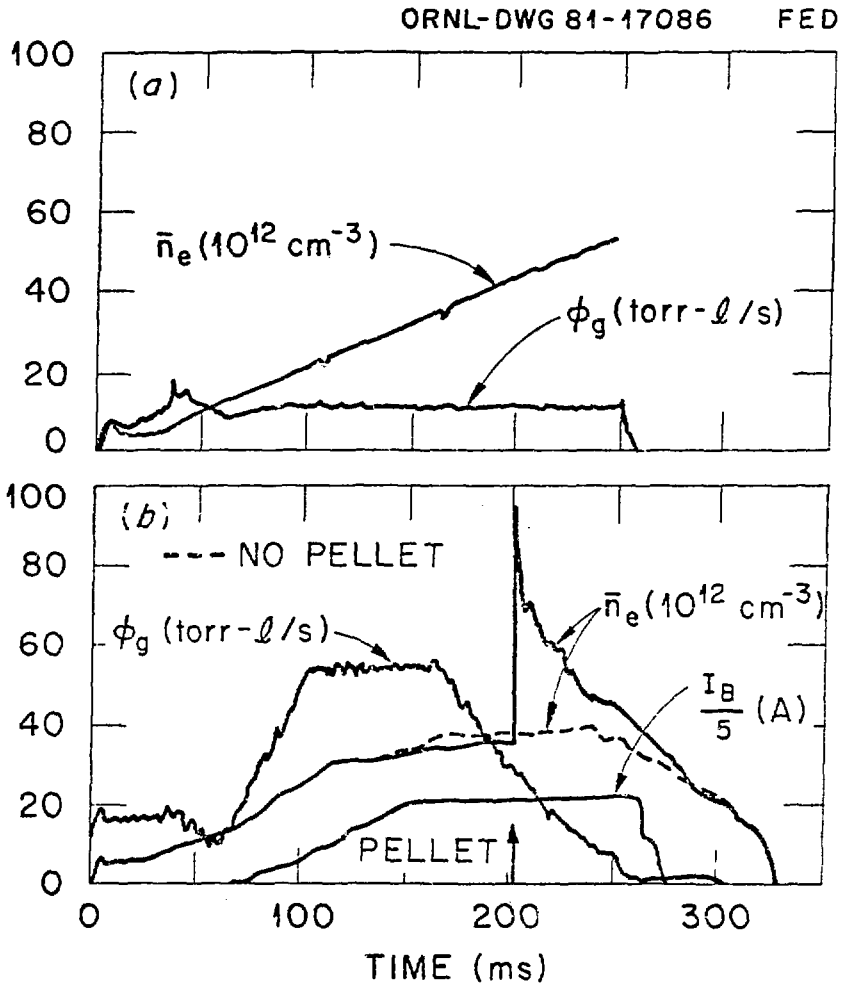
ORNL-DWG 81-17086 FED
(a)
$\bar{n}_e$ (10^{12} cm^{-3})
ϕ_g (torr-ℓ/s)
(b)
--- NO PELLET
ϕ_g (torr-ℓ/s)
$\bar{n}_e$ (10^{12} cm^{-3})
$\frac{I_B}{5}$ (A)
PELLET
TIME (ms)

MILORA
Fig. 3

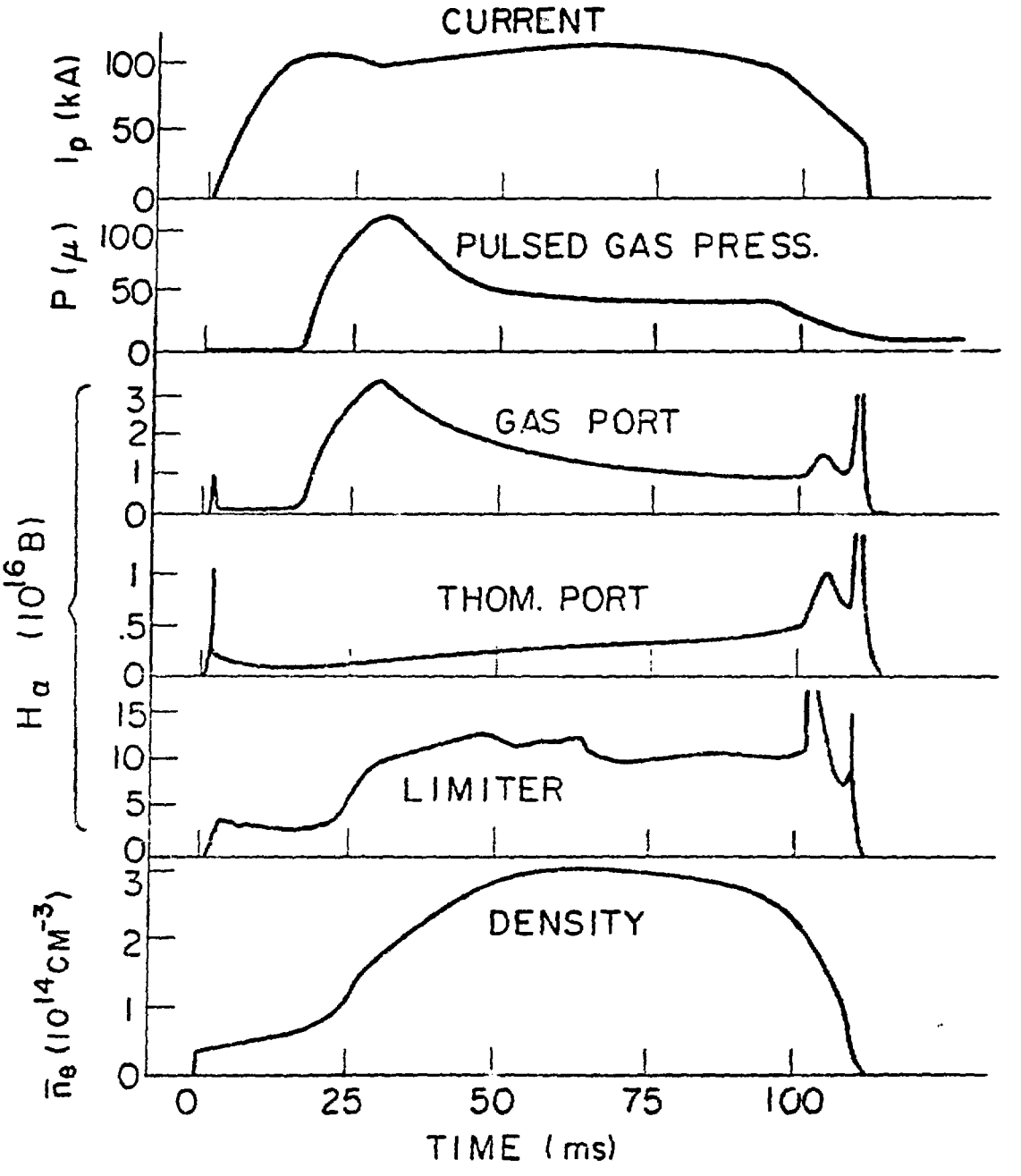
CURRENT
I_p (kA)
100
50
0
PULSED GAS PRESS.
P (μ)
100
50
0
GAS PORT
3
2
1
0
THOM. PORT
1
.5
0
LIMITER
15
10
5
0
H_α (10^{16}B)
DENSITY
3
2
1
0
$\bar{n}_e$ (10^{14}CM^{-3})
0
25
50
75
100
TIME (ms)

MILORA

Fig. 4

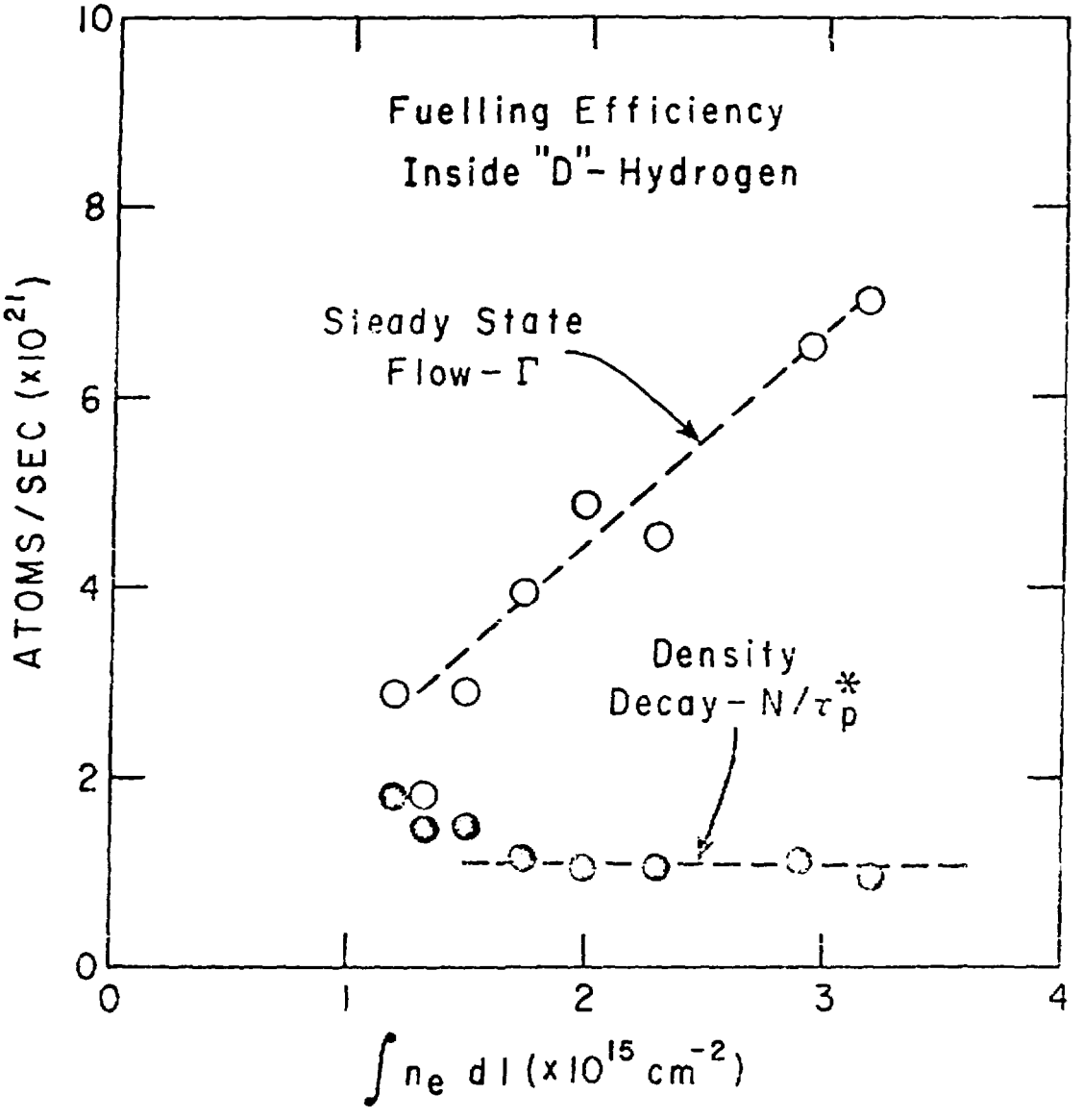
Fuelling Efficiency
Inside "D"- Hydrogen
Steady State
Flow - Γ
Density
Decay - N/τ*p
ATOMS/SEC (x10^21)
∫ ne dl (x10^15 cm^-2)
0
2
4
6
8
10
0
1
2
3
4

MILORA
Fig. 5

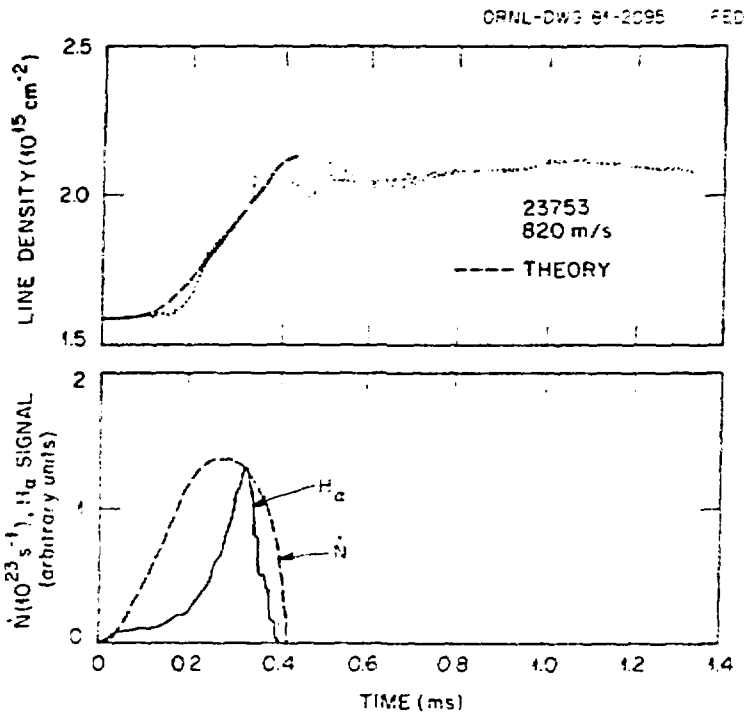
ORNL-DWG 81-2095 FED
LINE DENSITY (10^{15} cm^{-2})
2.5
2.0
1.5
23753
820 m/s
---- THEORY
$\dot{N}$ (10^{23} s^{-1}), H_α SIGNAL (arbitrary units)
2
0
H_α
$\dot{N}$
0
0.2
0.4
0.6
0.8
1.0
1.2
1.4
TIME (ms)

MILORA

Fig. 6

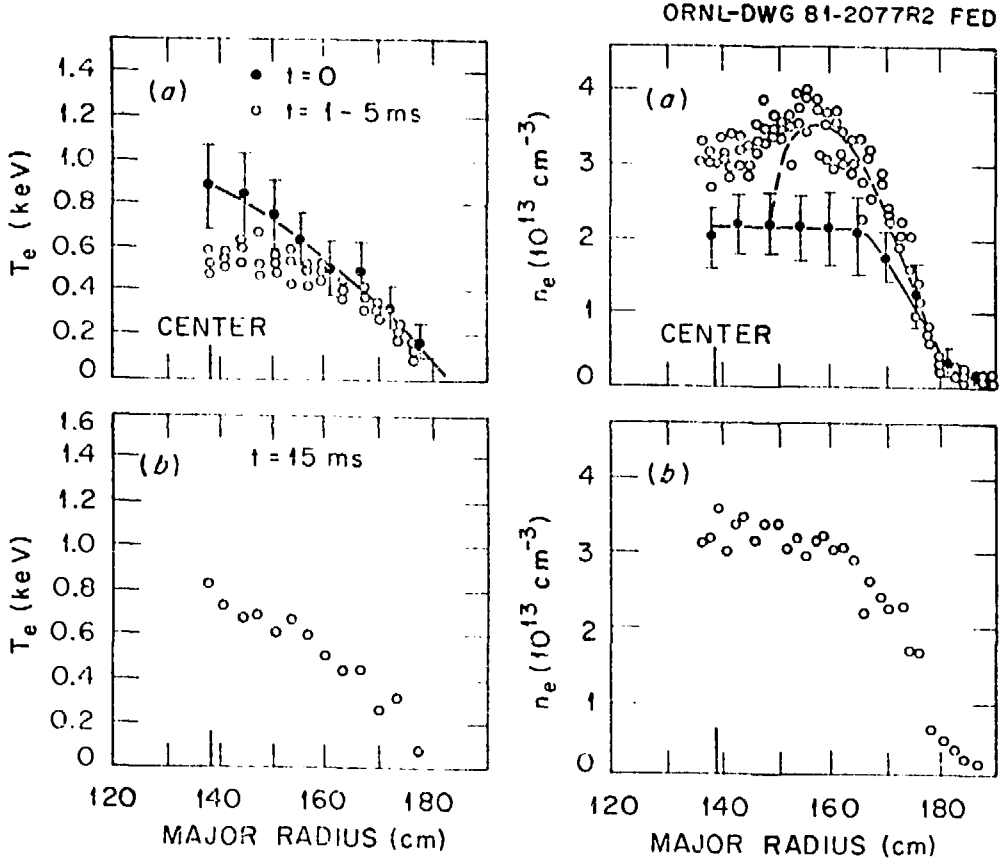
ORNL-DWG 81-2077R2 FED
(a)
t = 0
t = 1 - 5 ms
CENTER
(b)
t = 15 ms
T_e (keV)
n_e (10^{13} cm^{-3})
MAJOR RADIUS (cm)

MILORA

Fig. 7

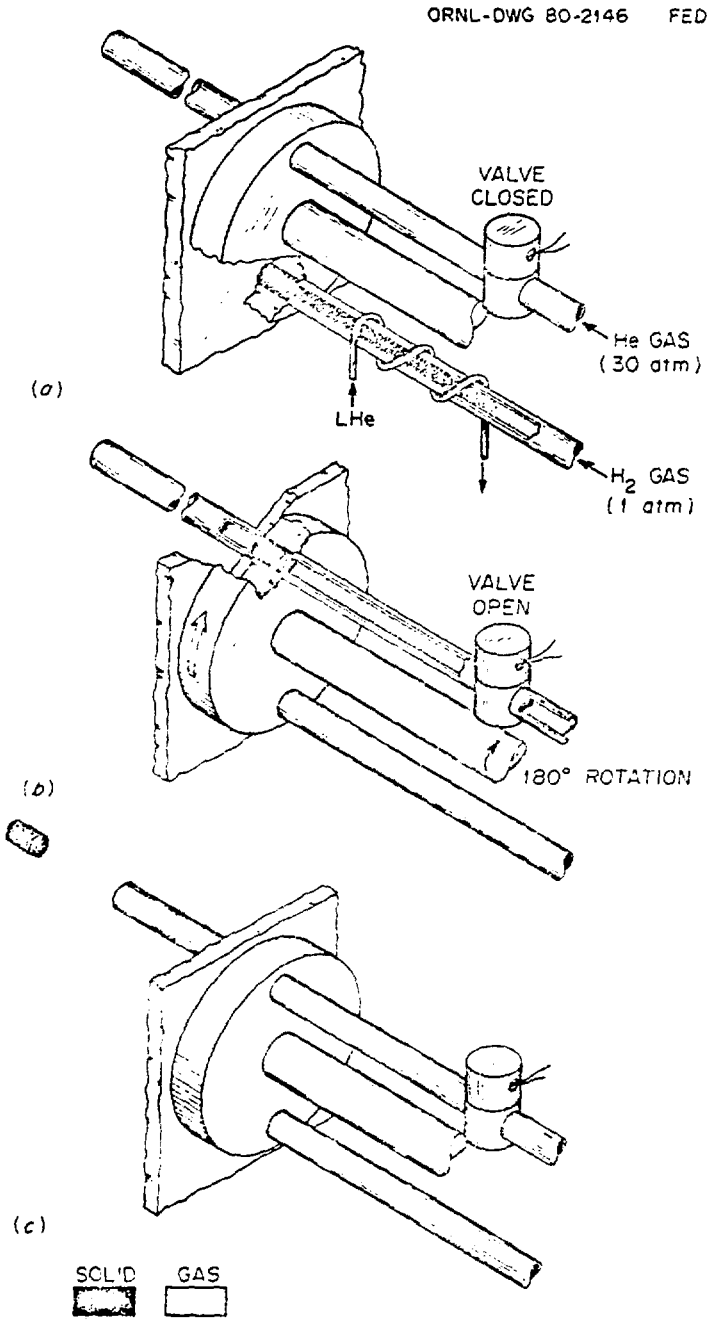
ORNL-DWG 80-2146 FED
VALVE CLOSED
He GAS (30 atm)
(a)
LHe
H_2 GAS (1 atm)
VALVE OPEN
(b)
180° ROTATION
(c)
SOL'D
GAS

MILORA

Fig. 8

MTLORA
Fig. 9

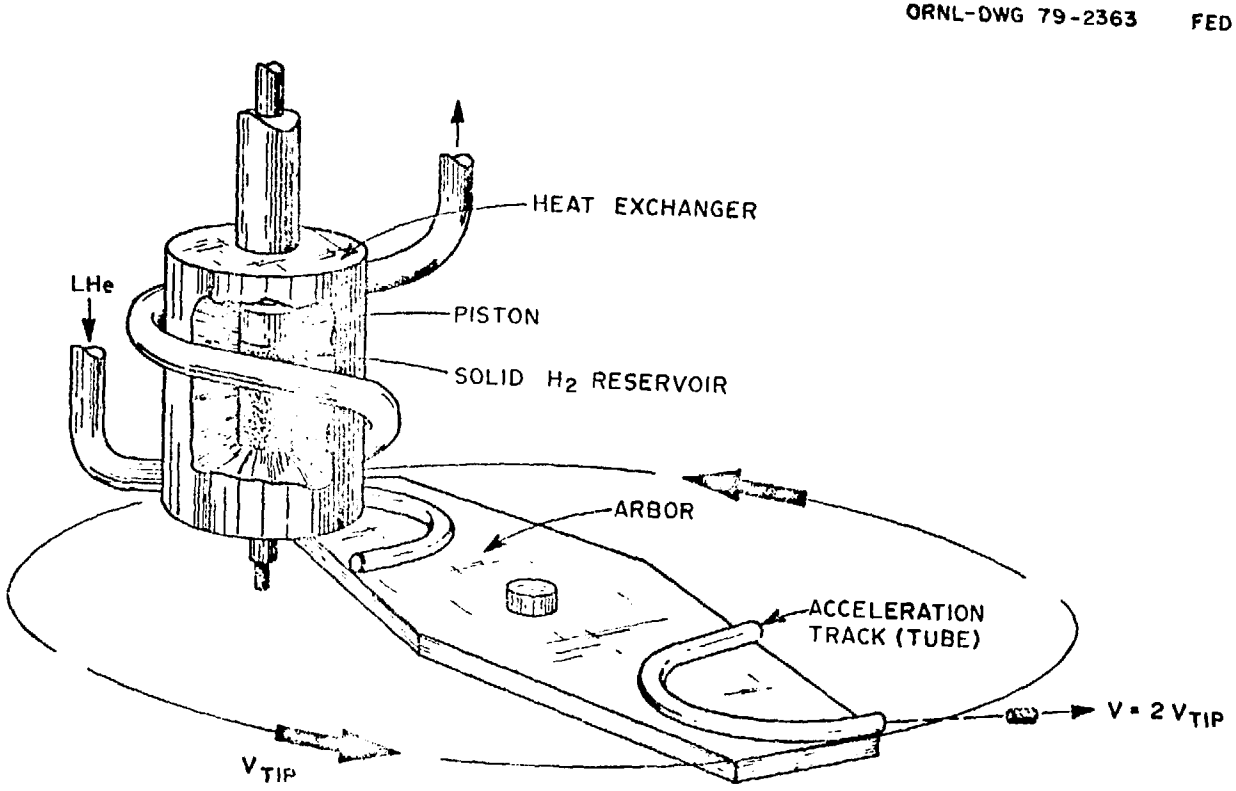
ORNL-DWG 79-2363 FED
HEAT EXCHANGER
LHe
PISTON
SOLID H_2 RESERVOIR
ARBOR
ACCELERATION TRACK (TUBE)
$V = 2V_{TIP}$
V_{TIP}

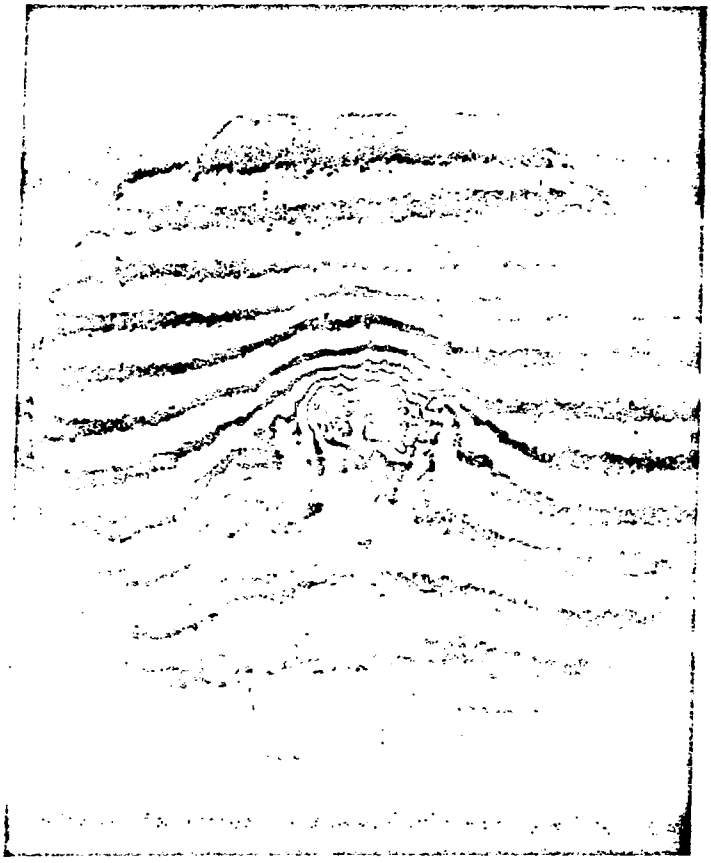

MILORA

Fig. 10

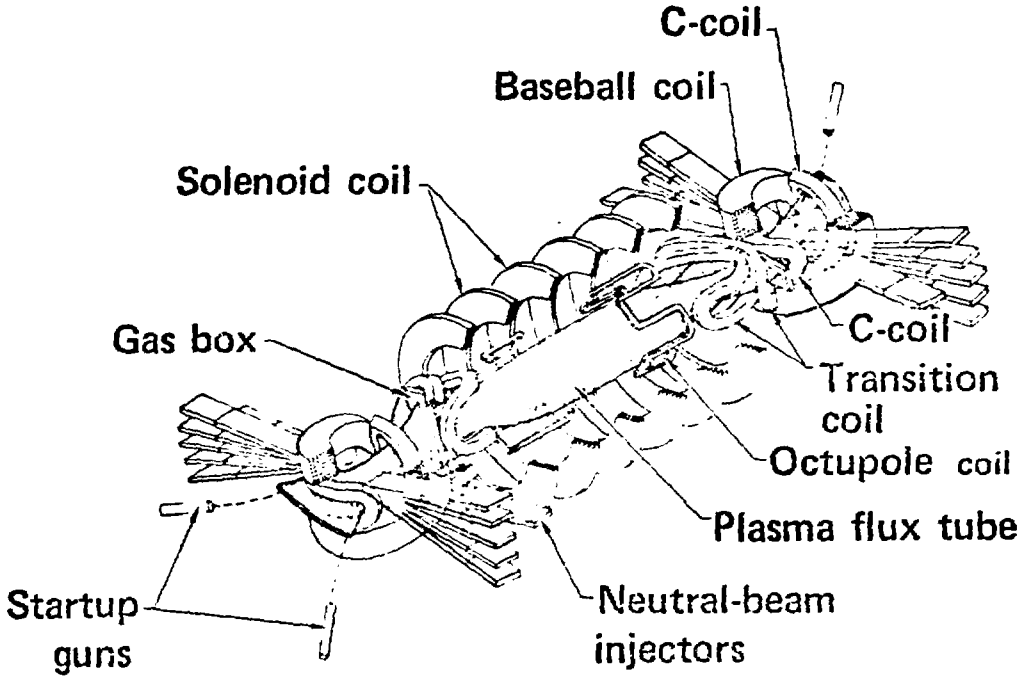

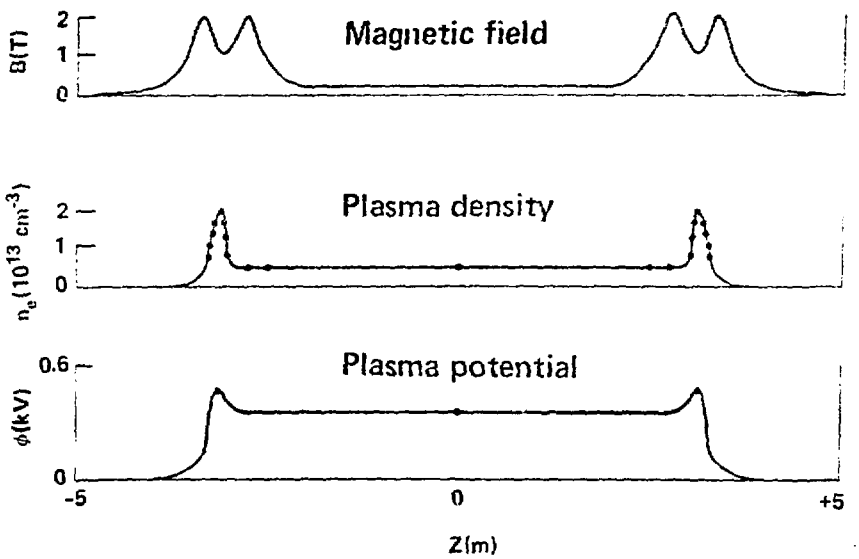

MILORA

Fig. 11